Automatic Segmentation of Brain Tissues and MR Bias Field Correction Using a Digital Brain Atlas

Koen Van Leemput, Frederik Maes, Dirk Vandermeulen, and Paul Suetens

Katholieke Universiteit Leuven, Medical Image Computing, Radiology-ESAT,
UZ Gasthuisberg, Herestraat 49, B-3000 Leuven, Belgium
Koen.VanLeemput@uz.kuleuven.ac.be

Abstract. This paper [1] proposes a method for fully automatic segmentation of brain tissues and MR bias field correction using a digital brain atlas. We have extended the EM segmentation algorithm, including an explicit parametric model of the bias field. The algorithm interleaves classification with parameter estimation, yielding better results at every iteration. The method can handle multi-channel data and slice-per-slice constant offsets, and is fully automatic due to the use of a digital brain atlas.

1 Introduction

Accurate segmentation of magnetic resonance (MR) images of the brain is of increasing interest in the study of many brain disorders such as schizophrenia and epilepsia. For instance, it is important to precisely quantify the total amounts of grey matter, white matter and cerebro-spinal fluid, as well as to measure abnormalities of brain structures. In multiple sclerosis, accurate segmentation of white matter lesions is necessary for drug treatment assessment. Since such studies typically involve vast amounts of data, manual segmentation is too time consuming. Furthermore, such manual segmentations show large inter- and intra-observer variability. Therefore, there is an increasing need for automated segmentation tools.

A major problem when segmenting MR images is the corruption with a smooth inhomogeneity bias field. Although not always visible for a human observer, such a bias field can cause serious misclassifications when intensity-based segmentation techniques are used.

Early methods for estimating and correcting bias fields used phantoms [1]. However, this approach assumes that the bias field is patient independent, which it is not. Homomorphic filtering [2] assumes that the frequency spectrum of the bias field and the image structures are well separated. This assumption, however, fails in the case of MR images. Other approaches use an intermediate classification or require that the user manually selects some reference points [3] [4].

[1] This paper is a short version of a technical report KUL/ESAT/PSI/9806 which can be obtained from the first author (Koen.VanLeemput@uz.kuleuven.ac.be)

Wells *et al.* [5] introduced the idea that estimation of the bias field is helped by classification and vice versa. This leads to an iterative method, interleaving classification with bias correction. In the Expectation-Maximization (EM) algorithm [6], which interleaves classification with class-conditional parameter estimation, Wells *et al.* substituted the step for estimating the class parameters by a bias estimation step. This requires that the user manually selects representative points for each of the classes considered. But such user interaction is time consuming, yields subjective and unreproducible segmentation results, and should thus be avoided if possible.

This paper describes a new method, based on the same idea of interleaving classification with bias correction. Rather than substituting the class-conditional parameter estimation step, as Wells *et al.* do, we propose an extension of the EM algorithm by including a bias field parameter estimation step. Furthermore, we use a digital brain atlas in the form of *a priori* probability maps for the location of the tissue classes. This method yields fully automatic classifications of brain tissues and MR bias field correction.

2 Method

2.1 The Expectation-Maximization (EM) algorithm

The EM algorithm [6] applied to segmentation interleaves a statistical classification of image voxels into K classes with estimation of the class-conditional distribution parameters. If each class is modeled by a normal distribution, then the probability that class j has generated the voxel value y_i at position i is $p(y_i \mid \Gamma_i{=}j, \theta_j) = G_{\sigma_j}(y_i - \mu_j)$ with $\Gamma_j \in \{j\}$ the tissue class at position i and $\theta_j = \{\mu_j, \sigma_j\}$ the distribution parameters for class j. Defining $\theta = \{\theta_j\}$ as the model parameters, the overall probability for y_i is

$$p(y_i \mid \theta) = \sum_j p(y_i \mid \Gamma_i{=}j, \theta_j) p(\Gamma_i{=}j)$$

The Maximum Likelihood estimates for the parameters μ_j and σ_j can be found by maximization of the likelihood $\prod_i p(y_i \mid \theta)$, equivalent to minimization of $\sum_i -\log(p(y_i \mid \theta))$. The expression for μ_j is given by the condition that

$$\frac{\partial}{\partial \mu_j} \left(\sum_i -\log \left(\sum_j p(y_i \mid \Gamma_i{=}j, \theta_j) p(\Gamma_i{=}j) \right) \right) = 0$$

Differentiating and using Bayes' rule

$$p(\Gamma_i{=}j \mid y_i, \theta) = \frac{p(y_i \mid \Gamma_i{=}j, \theta_j) p(\Gamma_i{=}j)}{\sum_j p(y_i \mid \Gamma_i{=}j, \theta_j) p(\Gamma_i{=}j)} \tag{1}$$

yields

$$\mu_j = \frac{\sum_i y_i \, p(\Gamma_i{=}j \mid y_i, \theta)}{\sum_i p(\Gamma_i{=}j \mid y_i, \theta)} \tag{2}$$

The same approach can be followed to find the expression for σ_j:

$$\sigma_j^2 = \frac{\sum_i p(\Gamma_i{=}j \mid y_i, \theta)(y_i - \mu_j)^2}{\sum_i p(\Gamma_i{=}j \mid y_i, \theta)} \tag{3}$$

Note that equation 1 performs a classification, whereas equation 2 and 3 are parameter estimates. Together they form a set of coupled equations, which can be solved by alternately iterating between classification and parameter estimation.

2.2 Extension of the EM algorithm

In order to estimate the bias field, we propose to make an extension of the EM algorithm. As in the original algorithm, each class j is modeled by a normal distribution, but now we also add a parametric model for the field inhomogeneity: the bias is modeled by a polynomial $\sum_k C_k \phi_k(x)$. Field inhomogeneities are known to be multiplicative; we first compute the logarithmic transformation on the intensities so that the bias becomes additive. Our model is then

$$p(y_i \mid \Gamma_i{=}j, \theta_j, C) = G_{\sigma_j}(y_i - \mu_j - \sum_k C_k \phi_k(x_i))$$

and

$$p(y_i \mid \theta, C) = \sum_j p(y_i \mid \Gamma_i{=}j, \theta_j, C) p(\Gamma_i{=}j)$$

with $C = \{C_k\}$ the bias field parameters. In order to find the bias field, the parameters μ_j, σ_j and C_k maximizing the likelihood $\prod_i p(y_i \mid \theta, C)$ must be searched. The C_k then allow calculating the estimated bias field.

Following the same approach as for equations 2 and 3, the expressions for the distribution parameters μ_j and σ_j are

$$\mu_j = \frac{\sum_i p(\Gamma_i{=}j \mid y_i, \theta, C)(y_i - \sum_k C_k \phi_k(x_i))}{\sum_i p(\Gamma_i{=}j \mid y_i, \theta, C)} \tag{4}$$

and

$$\sigma_j^2 = \frac{\sum_i p(\Gamma_i{=}j \mid y_i, \theta, C)(y_i - \mu_j - \sum_k C_k \phi_k(x_i))^2}{\sum_i p(\Gamma_i{=}j \mid y_i, \theta, C)} \tag{5}$$

Equations 4 and 5 are no surprise, as they are in fact the same equations which arise in the original EM algorithm (equations 2 and 3). The only difference is that the data is corrected for a bias field before the distribution parameters are calculated.

Setting the partial derivate for C_k to zero yields

$$\begin{bmatrix} C_1 \\ C_2 \\ \vdots \end{bmatrix} = (A^T W A)^{-1} A^T W \boldsymbol{r} \quad \text{with} \quad A = \begin{bmatrix} 1 & \phi_1(x_1) & \phi_2(x_1) & \cdots \\ 1 & \phi_1(x_2) & \phi_2(x_2) & \cdots \\ \vdots & \vdots & \vdots & \ddots \end{bmatrix} \tag{6}$$

and with weights W and residue $\boldsymbol{r}$

$$W_{mn} = \begin{cases} \sum_j \frac{p(\Gamma_m=j|y_m,\theta,C)}{\sigma_j^2} & \text{if } m = n \\ 0 & \text{otherwise} \end{cases} \qquad \boldsymbol{r} = \begin{bmatrix} y_1 - \frac{\sum_j p(\Gamma_1=j|y_1,\theta,C)\mu_j/\sigma_j^2}{\sum_j p(\Gamma_1=j|y_1,\theta,C)/\sigma_j^2} \\ y_2 - \frac{\sum_j p(\Gamma_2=j|y_2,\theta,C)\mu_j/\sigma_j^2}{\sum_j p(\Gamma_2=j|y_2,\theta,C)/\sigma_j^2} \\ \vdots \end{bmatrix}$$

Equation 6 is a weighted least-squares fit. From the intermediate classification and Gaussian distribution estimates, a prediction of the signal without bias is constructed and subtracted from the original data. A weight is assigned to each voxel of the resulting residue image, inversely proportional to a weighted variance. The bias is then the weighted least-squares fit to that residue. In the special case in which each voxel is exclusively assigned to one single class, the predicted signal contains the mean of the class each voxel belongs to. The weights are then inversely proportional to the variance of that class.

Iterating between equations 1, 4, 5 and 6 interleaves classification (step 1), distribution parameter estimation (step 2) and bias estimation (step 3). This has to be compared to the original EM algorithm, where only steps 1 and 2 were used. Wells *et al.* [5], on the contrary, only use steps 1 and 3.

2.3 Further extensions

We have further extended the algorithm to handle multi-channel data input. Furthermore, we have included a model for the background noise as well as for slice-per-slice constant offsets. We just summarize the results here; more details can be found in [7].

Multi-channel data The algorithm is easily extended to multi-channel data by substituting the Gaussian distributions by multivariate normals with mean $\boldsymbol{\mu}$ and covariance matrix Σ.

Background noise Since the background signal only contains noise and is not affected by the bias field, we have included an explicit model for the background noise. Pixels assigned to the background automatically get a zero weight for the bias estimation.

Slice-per-slice constant offsets In addition to a smoothly varying field inhomogeneity, 2D multi-slice sequence MR images, which are acquired in an interleaved way, are typically corrupted with additional slice-per-slice intensity offsets. We model these variations by assigning a 2D polynomial to each slice separately.

2.4 Digital brain atlas

In order to make the algorithm more robust and fully-automatic, a priori information is used in the form of an atlas. This atlas [8] contains a priori probability maps for white matter, grey matter and csf, as shown in figure 1.

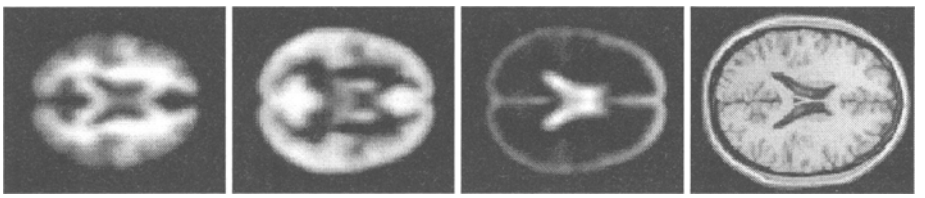

Fig. 1. The atlas consists of a priori probability maps for white matter, grey matter and csf, and a T1 template needed for registration of the subject to the space of the atlas

As a preprocessing step, we normalize the study images to the space of the atlas using the affine multi-modality registration technique described in [9]. At initialization, the atlas is used to sample the image for calculating the tissue-specific distribution parameters μ_j and σ_j. This approach frees us from interactively indicating representative pixels for each class. During subsequent iterations, the atlas is further used to spatially constrain the classification by using the spatially varying priors for $p(\Gamma_i{=}j)$ in equation 1. Thus, the voxels are not only classified based on their intensity, but also based on their spatial position. This makes the algorithm more robust, especially when the images are corrupted with a heavy bias field.

3 Results

We have implemented the algorithm as a modification of the SPM96 [10] segmentation tool, which originally used the EM algorithm without bias correction. We have performed experiments on various artificial and real MR data sets. In all the tests, a fourth order polynomial model for the bias was used. We here only shortly present some examples on real MR images of the head. A more detailed description can be found in [7], as well as some quantitative results on simulated MR data.

Single-channel data In figure 2, the classification of a high-resolution T1-weighted MR image is shown obtained with the EM algorithm without bias correction and with our extended EM algorithm using a 3D polynomial. For visualization purposes, we have made a hard segmentation from the probability maps by assigning each pixel exclusively to the class where it most probably belongs to. Because of a relatively strong bias field reducing the intensities in the slices at the top of the head, white matter is wrongly classified as the darker grey matter in those slices when the EM algorithm without bias correction is used. Our extended EM algorithm succeeds in compensating for this and provides better segmentations.

Multi-channel data The segmentation on a two-channel (PD and T2-weighted) MR image of the head is shown in figure 3. Although the effect of the bias field is hardly visible, it has a big impact on the resulting segmentation when the

EM algorithm without bias correction is used. With the extended algorithm, the segmentation is clearly improved.

MS lesion segmentation It is possible to assign multiple classes to the same a priori probability map. As an example, consider the problem of segmenting MS lesions. Since by far most of these lesions are located inside white matter, we have used the a priori white matter probability map for both the white matter and MS lesion class. The result for three-channel data of an MS patient, including T1, T2 and PD-weighted images, is shown in figure 4.

Slice-per-slice constant offsets As an example of bias correction for images with slice-per-slice constant offsets, we have processed the image shown in figure 5. The slice-per-slice offsets can clearly be seen as an interleaved bright-dark intensity pattern in a cross-section orthogonal to the slices. The estimated bias is also shown; it can be seen that the algorithm has found the slice-per-slice offsets.

4 Discussion

The algorithm that is proposed is based on Maximum-Likelihood parameter estimation using the EM algorithm. The method interleaves classification with parameter estimation, increasing likelihood at each iteration step.

The bias is estimated as a weighted least-squares fit, with the weights inversely proportional to the variance of the class each pixel belongs to. Since white matter and, in a lesser extend, grey matter have a narrow histogram, voxels belonging to the brain automatically get a large weight compared to non-brain tissues. We use a polynomial model for the bias field, which is a well-suited way for estimating bias fields in regions where the bias cannot be confidently estimated, i.e. regions with a low weight. The bias field is estimated from brain tissues and extrapolated to such regions.

At every iteration, the normal distribution parameters μ_j and σ_j for each class are updated. In combination with the atlas which provides a good initialization, this allows the algorithm to run fully automatic, avoiding manual selection of pixels representative for each of the classes considered. This yields objective and reproducible results. Furthermore, tissues surrounding the brain are hard to train for manually since they consist of a combination of different tissues types. Since our algorithm re-estimates the class distributions at each iteration, non-brain tissues automatically get a large variance and thus a low weight for the bias estimation.

We use an atlas which provides a priori information about the expected location of white matter, grey matter and csf. This information is used for initialization, avoiding user interaction which can give unreproducible results. Furthermore, the atlas makes the algorithm significantly more robust, since voxels are forced to be classified correctly even if the intensities largely differ due to a heavy bias field.

5 Summary and conclusions

In this paper, we have proposed a method for fully automatic segmentation of brain tissues and MR bias field correction using a digital brain atlas. We have extended the EM segmentation algorithm, including an explicit parametric model of the bias field. Results were presented on MR data with important field inhomogeneities and slice-per-slice offsets. The algorithm is fully automatic, avoids tedious and time-consuming user interaction and yields objective and reproducible results.

6 Acknowledgments

This research was performed within the context of the BIOMORPH project "Development and Validation of techniques for Brain Morphometry" supported by the European Commission under contract BMH4-CT96-0845 in the BIOMED2 programme and the research grant KV/E/197 (Elastische Registratie voor Medische Toepassingen) of the FWO-Vlaanderen to Dirk Vandermeulen.

References

1. M. Tincher, C.R. Meyer, R. Gupta, and D.M. Williams. Polynomial modeling and reduction of RF body coil spatial inhomogeneity in MRI. *IEEE transactions on medical imaging*, 12(2):361–365, june 1993.
2. R.C. Gonzalez and R.E. Woods. *Digital Image Processing.* Addison-Wesley, 1993.
3. Benoit M. Dawant, Alex P. Zijdenbos, and Richard A. Margolin. Correction of intensity variations in MR images for computer-aided tissue classification. *IEEE transactions on medical imaging*, 12(4):770–781, december 1993.
4. C.R. Meyer, P.H. Bland, and J. Pipe. Retrospective correction of MRI amplitude inhomogeneities. In N. Ayache, editor, *Proc. CVRMed '96, Computer Vision, Virtual Reality, and Robotics in Medicine; Lecture Notes in Computer Science*, pages 513–522. Berlin, Germany: Springer–Verlag, 1995.
5. W.M. Wells, III, W.E.L. Grimson, R. Kikinis, and F.A. Jolesz. Adaptive segmentation of MRI data. *IEEE transactions on medical imaging*, 15(4):429–442, august 1996.
6. A. P. Dempster, N. M. Laird, and D. B. Rubin. Maximum likelihood from incomplete data via the EM algorithm. *J. Roy. Stat. Soc.*, 39:1–38, 1977.
7. K. Van Leemput, D. Vandermeulen, and P. Suetens. Automatic segmentation of brain tissues and MR bias field correction using a digital brain atlas. Technical Report KUL/ESAT/PSI/9806, ESAT/PSI, june 1998.
8. Evans A.C., Collins D.L., Mills S.R., Brown E.D., Kelly R.L., and Peters T.M. 3d statistical neuroanatomical models from 305 MRI volumes. In *Proc. IEEE Nuclear Science Symposium and Medical Imaging Conference*, pages 1813–1817, 1993.
9. F. Maes, A. Collignon, D. Vandermeulen, G. Marchal, and P. Suetens. Multimodality image registration by maximization of mutual information. *IEEE transactions on medical imaging*, 16(2):187–198, april 1997.
10. John Ashburner, Karl Friston, Andrew Holmes, and Jean-Baptiste Poline. *Statistical Parametric Mapping.* The Wellcome Department of Cognitive Neurology, University College London.

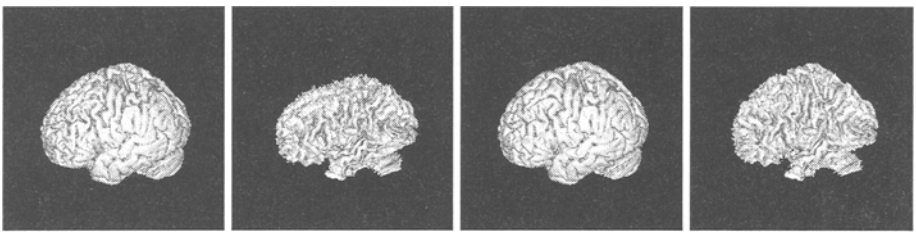

Fig. 2. 3D rendering of grey matter and white matter segmentations of a T1-weighted MR image of the head. From left to right: grey matter and white matter segmentation obtained with the EM algorithm without bias correction; grey matter and white matter segmentation obtained with the extended EM algorithm

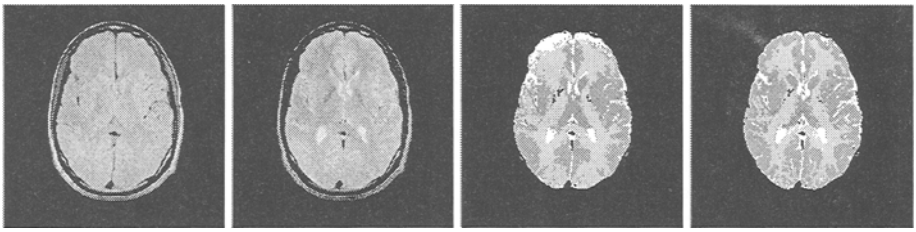

Fig. 3. Segmentation of multi-channel data. From left to right: PD and T2-weighted images, segmentation with the EM algorithm without bias correction and with the extended EM algorithm.

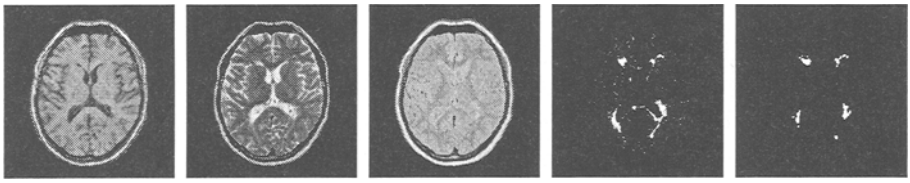

Fig. 4. MS lesion segmentation. From left to right: T1, T2, PD-weighted image, automatic lesion segmentation, manual segmentation

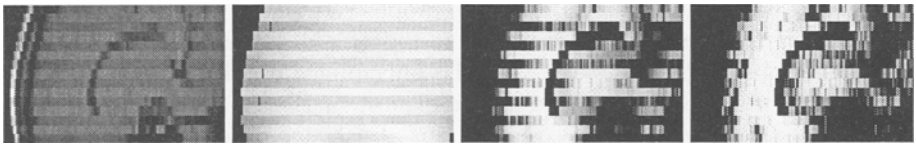

Fig. 5. An example of slice-per-slice offsets. From left to right: original data, estimated bias, white matter classification with the EM algorithm without bias correction and with the extended EM algorithm